Mitochondrial matrix delivery using a MITO-Porter, a liposome-based carrier that specifies fusion with mitochondrial membranes.

Yukari Yasuzaki[a, b], Yuma Yamada[a, b], Hideyoshi Harashima[a]*

[a] Laboratory for molecular design of pharmaceutics, Faculty of Pharmaceutical Sciences, Hokkaido University, Kita-12, Nishi-6, Kita-ku, Sapporo 060-0812, Japan

[b] These authors contributed equally as first author

*Corresponding author: Laboratory for molecular design of pharmaceutics, Faculty of Pharmaceutical Sciences, Hokkaido University, Kita-12, Nishi-6, Kita-ku, Sapporo 060-0812, Japan

Tel: +81-11-706-3919 Fax: +81-11-706-4879

E-mail: harasima@pharm.hokudai.ac.jp

Abstract Mitochondria are the principal producers of energy in cells of higher organisms. It was recently reported that mutations and defects in mitochondrial DNA (mtDNA) are associated with various mitochondrial diseases including a variety of neurodegenerative and neuromuscular diseases. Therefore, an effective mitochondrial gene therapy and diagnosis would be expected to have great medical benefits. To achieve this, therapeutic agents need to be delivered into the innermost mitochondrial space (mitochondrial matrix), which contains the mtDNA pool. We previously reported on the development of a MITO-Porter, a liposome-based carrier that introduces macromolecular cargos into mitochondria via membrane fusion. In this study, we provide a demonstration of mitochondrial matrix delivery and the visualization of mitochondrial genes (mtDNA) in living cells using the MITO-Porter. We first prepared a MITO-Porter containing encapsulated propidium iodide (PI), a fluorescent dye used to stain nucleic acids to detect mtDNA. We then confirmed the emission of red-fluorescence from PI by conjugation with mtDNA, when the carriers were incubated in the presence of isolated rat liver mitochondria. Finally, intracellular observation by confocal laser scanning microscopy clearly verified that the MITO-Porter delivered PI to the mitochondrial matrix.

Key words: Mitochondria; Mitochondrial matrix delivery; Mitochondrial drug delivery; Mitochondrial gene therapy; MITO-Porter; Membrane fusion; mtDNA.

Introduction

To date, a number of researchers have reported that genetic mutations of mitochondrial DNA (mtDNA) are associated with certain mitochondrial dysfunctions, which lead to a variety of human disorders including neurodegenerative and neuromuscular diseases[1;2;3;4;5;6;7]. For example, a mutation in mtDNA in the region encoding tRNA causes mitochondrial myopathy, encephalopathy, lactic acidosis and stroke-like episodes (MELAS)[8] and myoclonic epilepsy with ragged-red fibers (MERRF)[9]. In addition, deletions in mtDNA have been discovered in the majority of cases of chronic progressive external ophthalmoplegia (CPEO) and Kearms-Sayre syndrome (KSS) cases[10]. Therefore, an effective mitochondrial gene therapy and diagnosis would be a welcome event for many patients suffering from these intractable diseases. To achieve such an innovative strategy, in which the mitochondrial genome is the target, it is necessary to deliver therapeutic agents into the innermost mitochondrial space (the mitochondrial matrix), which contains the mtDNA pool.

Previous studies reported that the conjugation of mitochondrial targeting signal (MTS) peptides to exogenous proteins and small linear DNAs enhanced their delivery to mitochondria[11;12]. However, this strategy failed in cases where macromolecules and hydrophobic molecules, including mtDNA and mitochondrial proteins, were used, because the translocator for MTS severely restricts the size and physicochemical

property of the cargo[13;14;15]. To overcome this problem, we developed the MITO-Porter, a liposome-based carrier that permits macromolecular cargos to enter mitochondria via membrane fusion[16;17]. We first succeeded in identifying the lipid compositions that specify fusion with the mitochondrial membrane. Using living cells, we then showed that the MITO-Porter successfully delivered its cargo to the intra-mitochondrial compartment.

In this report, we provide evidence of mitochondrial matrix delivery using the MITO-Porter, as shown in Fig. 1. Propidium iodide (PI), a membrane-impermeable red-fluorescent dye for staining nucleic acids, was used as an aqueous phase marker for the MITO-Porter. This dye permits mitochondrial matrix delivery to be confirmed, by the detection of red-fluorescent light, because the light is emitted as the result of the conjugation of the dye with mtDNA in the mitochondrial matrix. We first confirmed mitochondrial matrix delivery in isolated rat liver mitochondria using the MITO-Porter. Confocal laser scanning microscopy (CLSM) analyses showed that this system can be used to efficiently visualize mtDNA, not only in isolated mitochondria, but in living cells as well. Finally, the fact the red fluorescence could be detected in living cells in spectral imaging fluorescent microscopy experiments clearly demonstrated that the MITO-Porter successfully delivered its cargo to the mitochondrial matrix.

Materials and methods

Materials.

1,2-Dioleoyl-sn-glycero-3-phosphatidyl ethanolamine (DOPE) and 7-nitrobenz-2-oxa-1,3-diazole labeled DOPE (NBD-DOPE) were purchased from Avanti Polar lipids (Alabaster, AL, USA). Egg yolk phosphatidyl choline (EPC) was obtained from Nippon Oil and Fats Co. (Tokyo, Japan). Sphingomyelin (SM) was purchased from Sigma (St. Louis, MO, USA). Stearyl octaarginine (STR-R8)[18] was obtained from KURABO INDUSTRIES LTD (Osaka, Japan). HeLa human cervix carcinoma cells were obtained from the RIKEN Cell Bank (Tsukuba, Japan). Dulbecco's modified Eagle medium (DMEM), Propidium iodide (PI), MitoTracker Deep Red 633 and Rhodamine123 were purchased from Molecular Probes (Eugene, OR, USA). 4', 6-diamidino-2-phenylindole (DAPI) was obtained from Wako Pure Chemical Industries, Ltd. (Osaka, Japan). Fetal bovine serum (FBS) was purchased from Thermo Scientific (Waltham, MA, USA). Adult male Wistar rats (6-10 weeks old) were purchased from Sankyo Labo Service (Sapporo, Japan). Mitochondria were isolated from rat livers essentially as described in the supplementary material. mtDNA was purified using previously reported protocols [19]. All other chemicals used were commercially available reagent-grade products.

Preparation of liposomes encapsulating PI.

Liposomes encapsulating PI (LPs [PI]) were prepared by the lipid film hydration method. Lipid films were produced on the bottom of a glass tube by the evaporation of a chloroform solution containing 1.38 μmol lipids for in vitro assays or 0.138 μmol lipids for cell imaging [DOPE/SM = 9 : 2 or EPC/SM = 9 : 2 (molar ratio)]. Next, 250 μL of 10 mM HEPES buffer (HB, pH 7.4) containing 0.1 mg of PI was applied to the lipid film, followed by incubation for 15 min at room temperature to hydrate the lipids. The lipid film was then sonicated for approximately 30 sec in a bath-type sonicator (85 W, Aiwa Co., Tokyo, Japan). The recovery ratio of PI was estimated as described in the Supplementary material. To attach R8 to the surface of the carrier, a solution of STR-R8 (10 mol% lipids) was added to the resulting suspensions. We refer to carriers with a mitochondrial fusogenic lipid composition [DOPE/SM/STR-R8 = 9 : 2 : 1 (molar ratio)] as a MITO-Porter, as described in our previous reports[16]. Particle diameters were measured using a quasi-elastic light scattering method, and ζ potentials were determined electrophoretically using laser doppler velocimetry (Zetasizer Nano ZS; Malvern Instruments, Herrenberg, Germany).

Evaluation of mitochondrial matrix targeting activity

The delivery of PI to the mitochondrial matrix by the MITO-Porter was confirmed by measuring the fluorescent intensity emitted from PI-mtDNA conjugates in the mitochondrial matrix. A 20-μL aliquot of PI, LPs [PI] and R8-modified LPs [PI] (final PI concentration, 0.08 mg/mL) were individually added to mitochondria isolated from rat liver (0.8 mg of mitochondrial protein/mL) in 80 μL of mitochondrial isolation buffer [MIB: 250 mM sucrose, 2 mM Tris-HCl, pH 7.4]. Immediately after mixing the suspension, time-lapse of its fluorescent intensity (excitation at 535 nm and emission at 617 nm) was measured within 10 min using an FP750 instrument (JASCO, Tokyo, Japan). Mitochondrial matrix targeting activities were calculated as follows:

$$\text{Mitochondrial matrix targeting activity} = (F_{10\text{min}} - F_{0\text{min}}) \quad (1)$$

where $F_{10\text{min}}$ and $F_{0\text{min}}$ represent the fluorescent intensity of each sample after incubation with mitochondria at 10 min and 0 min, respectively.

We also obtained fluorescent spectra of these samples to confirm that the source of the detected red fluorescence was PI-mtDNA conjugates. The spectra were obtained by measuring the fluorescent intensity in the range from 590 to 640 nm (excitation at 535 nm) using an FP750 instrument.

Visualization of the mitochondrial matrix delivery of PI by the MITO-Porter by confocal laser scanning microscopy

For the visualization of fluorescent light produced by PI-mtDNA conjugates in isolated mitochondria, after incubation with the MITO-Porter with encapsulated PI, the mitochondria were observed using a CLSM instrument. A 20-μL aliquot of R8-modified LPs [PI] (final PI concentration, 0.08 mg/mL) was individually incubated in a mitochondrial suspension (0.8 mg of mitochondrial protein/mL) for more than 10 min. An 80 μL aliquot of the resulting suspension was then incubated with Rhodamine123 in 400 μL of MIB for 15 min at 25ºC to stain the mitochondria (final concentration of Rhodamine123, 1 μg/mL). After the incubation, the suspension was centrifuged at 10,000*g* for 5 min at 4ºC to precipitate the mitochondria, and the supernatant was removed. The pellet was washed with MIB on ice, followed by resuspension in 100 μL of MIB. The mitochondrial suspension was embedded in Low melting point agarose gels (Seaplaque GTG agarose; BioWhittaker Molecular Applications, Rockland, ME, USA) as previously reported[20], and then observed by CLSM (Nikon A1; Nikon Co. Ltd., Tokyo, Japan). The mitochondria were excited with 488 nm wavelength light from an Ar laser and 561 nm wavelength light from a DPSS laser. A series of images were obtained using a Nikon A1 confocal imaging system equipped with a water immersion

objective lens (Plan Apo 60x1.20 PFS WI) and a 1st dichroic mirror (405/488/561/640). The two fluorescence detection channels (Ch) were set to the following filters: 525/50 (green) and 595/50 (red).

MITO-Porter transduction into living cells and intracellular observation by confocal laser scanning microscopy

The MITO-Porter with encapsulated PI was incubated with HeLa cells to observe the fluorescent emission produced by the PI-mtDNA conjugates (Fig. 3A). HeLa cells (4 x 10^4 cells) were cultured in 35 mm glass base dishes (IWAKI, Tokyo, Japan) with D'MEM, which contained 10% FBS, under 5% CO_2/air at 37ºC for 24 ± 4 hr. R8-modified LPs [PI] (final lipid concentration, 50 μM) were added to the HeLa cells in phenol red-free medium without serum and incubated under 5% CO_2/air at 37ºC. After a 1-hr incubation, the medium was replaced with fresh phenol red-free medium containing serum, and the cells were incubated in the absence of the carriers. After a further 1.5 hr, the medium was replaced with fresh medium containing Rhodamine123 (final concentration, 100 ng/mL) and the cells were incubated for an additional 30 min to allow the mitochondria to be stained. After this incubation, the cells were washed with the phenol red-free medium containing serum, and then observed by a CLSM

(Nikon A1) in a similar setting as described above.

We also observed the intracellular trafficking of the MITO-Porter. PI encapsulated in the MITO-Porter labeled with NBD-DOPE, as a tracer of the carrier, was incubated with HeLa cells. The medium was then replaced with fresh medium containing MitoTracker Deep Red 633 (final concentration, 100 nM) and the cells were incubated for a further 30 min to permit the mitochondria to be stained. The cells were excited by a 488 nm light from an Ar laser, 561 nm light from a DPSS laser and 640 nm light from a Diode laser. A series of images were obtained using a Nikon A1 equipped with a water immersion objective lens (Plan Apo 60x1.20 PFS WI) and a 1st dichroic mirror (405/488/561/640). The three fluorescence detection channels (Ch) were set to the following filters: 525/50 (green), 595/50 (red) and 700/75 (blue pseudo color).

Validation of PI binding to mtDNA in isolated mitochondria and in living cells using spectral imaging fluorescent microscopy

As described above, the MITO-Porter with encapsulated PI was incubated with isolated rat liver mitochondria or living cells, and these were then observed using a Nikon A1 microscope equipped with a water immersion objective lens (Plan Apo 60x1.20 PFS WI). To confirm that the red dots shown in the images in Fig 3A are

derived from PI-mtDNA conjugates, spectral images were obtained ranging from 582 to 750 nm with a DPSS laser (561 nm) using a 1st dichroic mirror (405/488/561). Fluorescence spectra of the R.O.I. (region of image) were selected Fig. 3B (a) and the emission at each wavelength was normalized to the peak fluorescence intensity, as shown in Fig. 3B (b).

Results and discussion

Preparation of a MITO-Porter for the detection of mtDNA.

To detect mtDNA, probes must reach the mitochondrial matrix, which contains the mtDNA pool. In this study, we attempted to deliver a cargo to the mitochondrial matrix using the MITO-Porter. We utilized PI (an impermeable fluorescence-dye for nucleic acids) as a probe to detect mtDNA, and encapsulated it in the aqueous phase of the MITO-Porter. In this strategy, PI would emit a red fluorescence only after conjugation with mtDNA in the mitochondrial matrix, because PI cannot pass through a cell membrane or mitochondrial membranes. We prepared liposomes with encapsulated PI by the hydration method, and determined their diameters and zeta potentials (Table S1 in supplementary material). The diameters were comparable (approximately 200-400 nm). The zeta potentials of the R8-modified LPs were positively charged, indicating that the surface of the carrier was modified with R8.

Evaluation of mitochondrial matrix targeting activity and visualization of mtDNA.

Liposomes encapsulating PI were incubated with isolated rat liver mitochondria, and their matrix targeting activity evaluated by measuring the fluorescent intensity emitted from PI-mtDNA conjugates. We first confirmed that PI emitted a red

fluorescence when conjugated with mtDNA (Fig. S1 in supplementary material). As shown in Fig 2A, the MITO-Porter, which has a mitochondrial fusogenic lipid composition, showed a higher matrix targeting activity than other carriers. This result suggests that the MITO-Porter has the ability to deliver PI to the mitochondrial matrix and that it can be used to detect mtDNA. On the other hand, carriers with a low mitochondrial fusion activity showed a lower matrix targeting activity. The matrix targeting activities of the R8-unmodified carriers were as low as the level observed for PI only. We also obtained a fluorescence spectrum of a mitochondrial suspension incubated with the MITO-Porter with encapsulated PI (Fig. 2B). The findings confirmed that the resulting spectrum was similar to that for PI mixed with mtDNA.

We next visualized mtDNA after the mitochondrial matrix delivery of PI via the MITO-Porter. The mitochondria were stained with Rhodamine123, as a probe of mitochondrial membrane potential[21;22], prior to observation by CLSM. In the case of the MITO-Porter, strong red signals were detected (Fig. 2C (a)), and these signals were observed to be co-localized with mitochondria, as can be seen by the yellow signal in the merged images (Fig. 2C (c)). These results suggest that the MITO-Porter successfully delivered a cargo to the mitochondrial matrix with the mitochondrial membrane potential being maintained. In contrast, only faint red signals were observed

in the case of a carrier with a low mitochondrial fusion activity (Fig. 2C (d)). We also confirmed that no red signal was observed, when carrier only or PI only were incubated with mitochondria (Fig. S2 (A-F) in supplementary material). Moreover, we confirmed that the red fluorescence spectral curve was due to PI conjugated with nucleic acids by spectral imaging fluorescent microscopy (Fig. 2D).

Validation of mitochondrial matrix delivery in living cells by MITO-Porter.

To validate the delivery of the MITO-Porter to the mitochondrial matrix, PI encapsulated in the MITO-Porter was incubated with HeLa cells, and intracellular trafficking was observed by CLSM. When living cells were treated with PI only or carrier only, no red signals were observed in the cells (Fig. S3 (A-F) in supplementary material). In the case of the MITO-Porter, however, several strong red-signals were detected (Fig. 3A (a)), and these signals were observed to be co-localized with mitochondria (Fig. 3A (b)). On the other hand, no red-signals were detected in the case of carriers with low mitochondrial fusion activity (Fig. S3 (J-L) in supplementary material). In addition, we identified the spectral curve for the observed red fluorescence as that of PI conjugated with nucleic acids (Fig. 3B).

We expected to see many red-signals on mitochondria in living cells; however,

only a few red signals were observed (Fig. 3A (a)). These results can be explained by the fact that the staining of mtDNA by a fluorescent dye is more difficult than the staining of nucleic acids in nuclei. Since one mitochondrion contains only a small amount of nucleic acid (mtDNA) compared with a nucleus, the concentration of mtDNA-PI conjugates might be too low to permit their visualization. To validate this hypothesis, we carried out the staining mtDNA in living cells using DAPI, a well known nuclear and chromosome counterstain. It has been reported that nucleic acids in both the nucleus and mitochondria are stained, when cells are treated with high concentrations of DAPI[23] (see the supplementary material for the details).

HeLa cells were incubated with a high concentration of DAPI (final concentration, 15 μg/mL) for 30 min to stain the nucleic acids (cyan pseudo color). The mitochondria were then stained with Rhodamine123 (red pseudo color), followed by observation by CLSM. Under the conditions described above, the saturation of fluorescence produced by DAPI-nucleic acid conjugates in the nucleus was observed (Fig.3C). The white colored signals correspond to DAPI conjugated with mtDNA colocalized with mitochondria. On the other hand, in the case of optimal conditions for nuclear staining (less than 2 μg/mL of DAPI, 5-min incubation), no fluorescence derived from DAPI-mtDNA conjugates was observed (data not shown). Taking these

results into consideration, the detection of mtDNA by the MITO-Porter can be accomplished. The above findings confirm that the MITO-Porter has the ability to deliver PI to the mitochondrial matrix, resulting in the successful detection of mtDNA in living cells.

Intracellular observation of MITO-Porter and detection of mtDNA using confocal laser scanning microscopy.

PI encapsulated in the MITO-Porter labeled with NBD-DOPE (green color) as a tracer of the carrier were incubated with HeLa cells. The mitochondria were stained with MitoTracker Deep Red 633 prior to intracellular observation (blue pseudo color). Figure 4D shows a typical merged image of the florescence. Red/pink clusters, as indicated by (i), represent PI conjugated with mtDNA. Yellow/white clusters, as indicated by (ii) or (iii), represent PI conjugated with nucleic acids (red) and colocalized with the lipids of carriers that had accumulated in mitochondria or the nucleus (green). Green/cyan, as indicated by (iv), represent carrier only.

Most of the red signals were observed in mitochondria (i). Yellow/white clusters (ii), corresponding to the accumulation of the lipids associated with carriers (green) in mitochondria, were observed. We also observed yellow signals in the nucleus

(iii). The MITO-Porter might be taken up by the nucleus during cell division. The fact that no yellow clusters were observed without mitochondria suggest that PI emits a red fluorescence only after it is delivered to mitochondria. The presence of green/cyan clusters on mitochondria (iv) suggests that an insufficient amount of PI was delivered to the mitochondrial matrix to permit the visualization of mtDNA, or the green signals of the carriers may be too strong compared with the red signals. These results support the conclusion that the MITO-Porter delivers cargoes to the mitochondrial matrix, which contains the mtDNA pool.

Conclusion

In this study, we report on the successful visualization of mtDNA in living cells using MITO-Porter. The findings indicate that the MITO-Porter has the ability to deliver cargoes to the mitochondrial matrix. As a result, the system has the potential to be used in gene therapy and diagnosis of mitochondrial diseases.

Acknowledgments

This work was supported in part by Grant-in-Aid for Young Scientists (B) from the Ministry of Education, Culture, Sports, Science and Technology of Japanese Government. We also thank Dr. Milton Feather for his helpful advice in writing the manuscript.

References

[1] S. DiMauro, Mitochondrial myopathies. Curr Opin Rheumatol 18 (2006) 636-41.

[2] I.J. Holt, A.E. Harding, and J.A. Morgan-Hughes, Deletions of muscle mitochondrial DNA in patients with mitochondrial myopathies. Nature 331 (1988) 717-9.

[3] Y. Kagawa, Y. Inoki, and H. Endo, Gene therapy by mitochondrial transfer. Adv Drug Deliv Rev 49 (2001) 107-19.

[4] L.J. Martin, Mitochondriopathy in Parkinson disease and amyotrophic lateral sclerosis. J Neuropathol Exp Neurol 65 (2006) 1103-10.

[5] E. Sarzi, M.D. Brown, S. Lebon, D. Chretien, A. Munnich, A. Rotig, and V. Procaccio, A novel recurrent mitochondrial DNA mutation in ND3 gene is associated with isolated complex I deficiency causing Leigh syndrome and dystonia. Am J Med Genet A 143 (2007) 33-41.

[6] D.C. Wallace, Mitochondrial diseases in man and mouse. Science 283 (1999) 1482-8.

[7] D.C. Wallace, The mitochondrial genome in human adaptive radiation and disease: on the road to therapeutics and performance enhancement. Gene 354 (2005) 169-80.

[8] Y. Goto, I. Nonaka, and S. Horai, A mutation in the tRNA(Leu)(UUR) gene associated with the MELAS subgroup of mitochondrial encephalomyopathies. Nature 348 (1990) 651-3.

[9] J.M. Shoffner, M.T. Lott, A.M. Lezza, P. Seibel, S.W. Ballinger, and D.C. Wallace, Myoclonic epilepsy and ragged-red fiber disease (MERRF) is associated with a mitochondrial DNA tRNA(Lys) mutation. Cell 61 (1990) 931-7.

[10] S. Shanske, C.T. Moraes, A. Lombes, A.F. Miranda, E. Bonilla, P. Lewis, M.A. Whelan, C.A. Ellsworth, and S. DiMauro, Widespread tissue distribution of mitochondrial

DNA deletions in Kearns-Sayre syndrome. Neurology 40 (1990) 24-8.

[11] A. Flierl, C. Jackson, B. Cottrell, D. Murdock, P. Seibel, and D.C. Wallace, Targeted delivery of DNA to the mitochondrial compartment via import sequence-conjugated peptide nucleic acid. Mol Ther 7 (2003) 550-7.

[12] G. Schatz, The protein import system of mitochondria. J Biol Chem 271 (1996) 31763-6.

[13] T. Endo, Y. Nakayama, and M. Nakai, Avidin fusion protein as a tool to generate a stable translocation intermediate spanning the mitochondrial membranes. J Biochem (Tokyo) 118 (1995) 753-9.

[14] M. Esaki, T. Kanamori, S. Nishikawa, and T. Endo, Two distinct mechanisms drive protein translocation across the mitochondrial outer membrane in the late step of the cytochrome b(2) import pathway. Proc Natl Acad Sci U S A 96 (1999) 11770-5.

[15] A. Gruhler, H. Ono, B. Guiard, W. Neupert, and R.A. Stuart, A novel intermediate on the import pathway of cytochrome b2 into mitochondria: evidence for conservative sorting. Embo J 14 (1995) 1349-59.

[16] Y. Yamada, H. Akita, H. Kamiya, K. Kogure, T. Yamamoto, Y. Shinohara, K. Yamashita, H. Kobayashi, H. Kikuchi, and H. Harashima, MITO-Porter: A liposome-based carrier system for delivery of macromolecules into mitochondria via membrane fusion. Biochim Biophys Acta 1778 (2008) 423-32.

[17] Y. Yamada, H. Akita, K. Kogure, H. Kamiya, and H. Harashima, Mitochondrial drug delivery and mitochondrial disease therapy - An approach to liposome-based delivery targeted to mitochondria. Mitochondrion 7 (2007) 63-71.

[18] S. Futaki, W. Ohashi, T. Suzuki, M. Niwa, S. Tanaka, K. Ueda, H. Harashima, and Y. Sugiura, Stearylated arginine-rich peptides: a new class of transfection systems. Bioconjug Chem 12 (2001) 1005-11.

[19] T.K. Palva, and E.T. Palva, Rapid isolation of animal mitochondrial DNA by alkaline extraction. FEBS Lett 192 (1985) 267-70.

[20] S. Meeusen, J.M. McCaffery, and J. Nunnari, Mitochondrial fusion intermediates revealed in vitro. Science 305 (2004) 1747-52.

[21] L.V. Johnson, M.L. Walsh, and L.B. Chen, Localization of mitochondria in living cells with rhodamine 123. Proc Natl Acad Sci U S A 77 (1980) 990-4.

[22] R.C. Scaduto, Jr., and L.W. Grotyohann, Measurement of mitochondrial membrane potential using fluorescent rhodamine derivatives. Biophys J 76 (1999) 469-77.

[23] T. Ozawa, Y. Natori, M. Sato, and Y. Umezawa, Imaging dynamics of endogenous mitochondrial RNA in single living cells. Nat Methods 4 (2007) 413-9.

Figure legends

Figure 1. Schematic diagram for the detection of mtDNA in living cells using a MITO-Porter encapsulating PI.

The MITO-Porter is surface-modified with a high density of R8, which can be internalized by cells via macropinocytosis (1st step). The MITO-Porter can escape from macropinosomes to the cytosol (2nd step). The MITO-Porter in the cytosol can bind to mitochondria via electrostatic interactions with R8 (3rd step). Encapsulated compounds are delivered to the intra-mitochondrial compartment via membrane fusion (4th step). Finally, PI forms conjugates with mtDNA, which emit red-fluorescent light (5th step). DOPE, 1,2-dioleoyl-sn-glycero-3-phosphatidyl ethanolamine; SM, sphingomyelin; STR-R8, stearyl R8.

Figure 2. Evaluation of mitochondrial matrix targeting activity and the visualization of mtDNA using MITO-Porter.

A, Mitochondrial matrix targeting activities of various carriers were estimated using isolated rat liver mitochondria. Bars represent the mean values (n = 4-9). **Significant difference ($p < 10^{-9}$) and *Significant difference ($p < 10^{-4}$) were calculated by one-way ANOVA, followed by the Bonferroni correction post hoc test.

B, Fluorescence spectrum of mitochondrial suspension incubated with MITO-Porter encapsulating PI was obtained (closed circles). We also measured the fluorescent spectrum of PI mixed with mtDNA (open circles).

C, mtDNA in isolated rat liver mitochondria was visualized using confocal laser scanning microscopy: PI encapsulated in the MITO-Porter (a-c) or a control carrier with low mitochondrial fusion activity (d-f). Mitochondria were stained with Rhodamine123 prior to observation: (left panels; red) PI, (middle panels; green) Rhodamine123, and (right panels) merge images. Note that PI appeared as yellow clusters when it was localized in mitochondrial matrix to conjugate with mtDNA. Scale bars, 10 μm.

D, Fluorescence spectra of R.O.I. (region of image) were selected from Fig2. C (a) and the emission were normalized to the PI peak fluorescence intensity (blue line indicated by 1). The spectra of PI mixed with nucleic acids (provided by Nikon Co. Ltd) the present red line indicted by 2.

Figure 3. Validation of mitochondrial matrix delivery in living cells by the MITO-Porter.

A, PI encapsulated in MITO-Porter was incubated with HeLa cells, and the mitochondria were stained with Rhodamine123 (green) prior to observation by confocal

laser scanning microscopy: overlay image (a). Note that PI emits a red-fluorescent signal when conjugated with nucleic acids. To confirm the colocalization of PI-fluorescence and mitochondria, the fluorescent intensities of both PI (red line) and Rhodamine123 (green line) were estimated from (i) to (ii) in the inset image 1 (b). Scale bar, 10 μm.

B, Fluorescent spectral data for PI encapsulated in the MITO-Porter in living cells were collected. (**a**) Fluorescent overlay images were observed under conditions similar to those shown in Fig.3A. (**b**) Fluorescence spectra of R.O.I. (region of image) were selected from Fig. 3B (a) and the emissions were normalized to the PI peak fluorescence intensity. The R.O.I. on and outside the mitochondria are indicated by X or Y, respectively. The spectra of PI mixed with nucleic acids (provided by Nikon Co. Ltd) shown as a white line indicted by Z. Scale bar, 10 μm.

C, Nucleic acids within nuclei and mitochondria in living cells were staining with DAPI (cyan pseudo color). Prior to the observations, the mitochondria were stained with Rhodamine123 (red pseudo color). Scale bar, 10 μm.

Figure 4. Intracellular observation of MITO-Porter and detection of mtDNA.

PI encapsulated in MITO-Porter labeled with NBD-DOPE as a tracer of the carrier were

incubated with HeLa cells. The mitochondria were stained with MitoTracker Deep Red 633 prior to intracellular observation: (A; green color) NBD-DOPE, (B; red color) PI conjugated with nucleic acids, (C; blue pseudo color) Mito Tracker Deep Red 633, and (D) merge images. Red arrows, as indicated by (i), PI conjugated with mtDNA. Yellow arrows, as indicated by (ii), show that PI conjugated with mtDNA (red) is colocalized with the lipids of carriers that had accumulated in mitochondria (green). White arrow, as indicated by (iii), show that PI conjugated with nucleic acids in nucleus (red) is colocalized with the lipids of carriers accumulated in nucleus (green). Green arrows, as indicated by (iv), show carrier on mitochondria (cyan) or outside mitochondria (green). Scale bars, 10 μm.

Figure 1

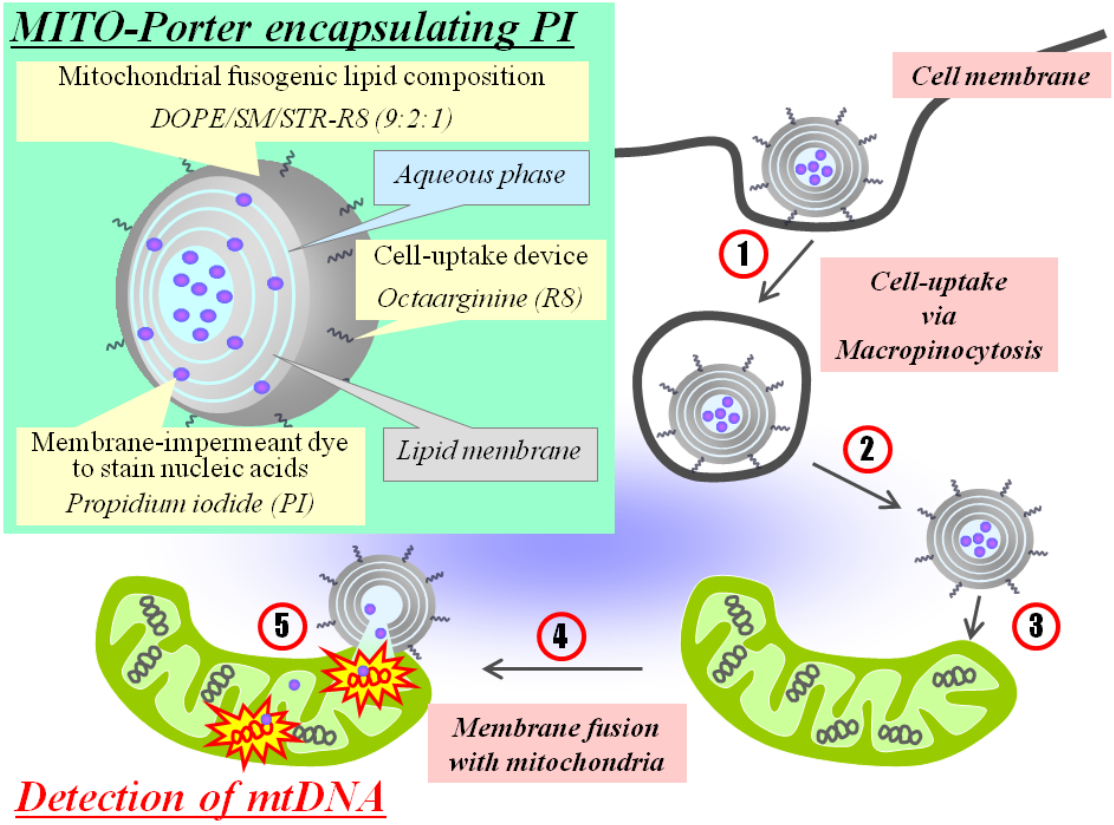
MITO-Porter encapsulating PI
Mitochondrial fusogenic lipid composition
DOPE/SM/STR-R8 (9:2:1)
Aqueous phase
Cell-uptake device
Octaarginine (R8)
Membrane-impermeant dye
to stain nucleic acids
Propidium iodide (PI)
Lipid membrane
Cell membrane
1
Cell-uptake
via
Macropinocytosis
2
3
4
5
Membrane fusion
with mitochondria
Detection of mtDNA

Figure 2

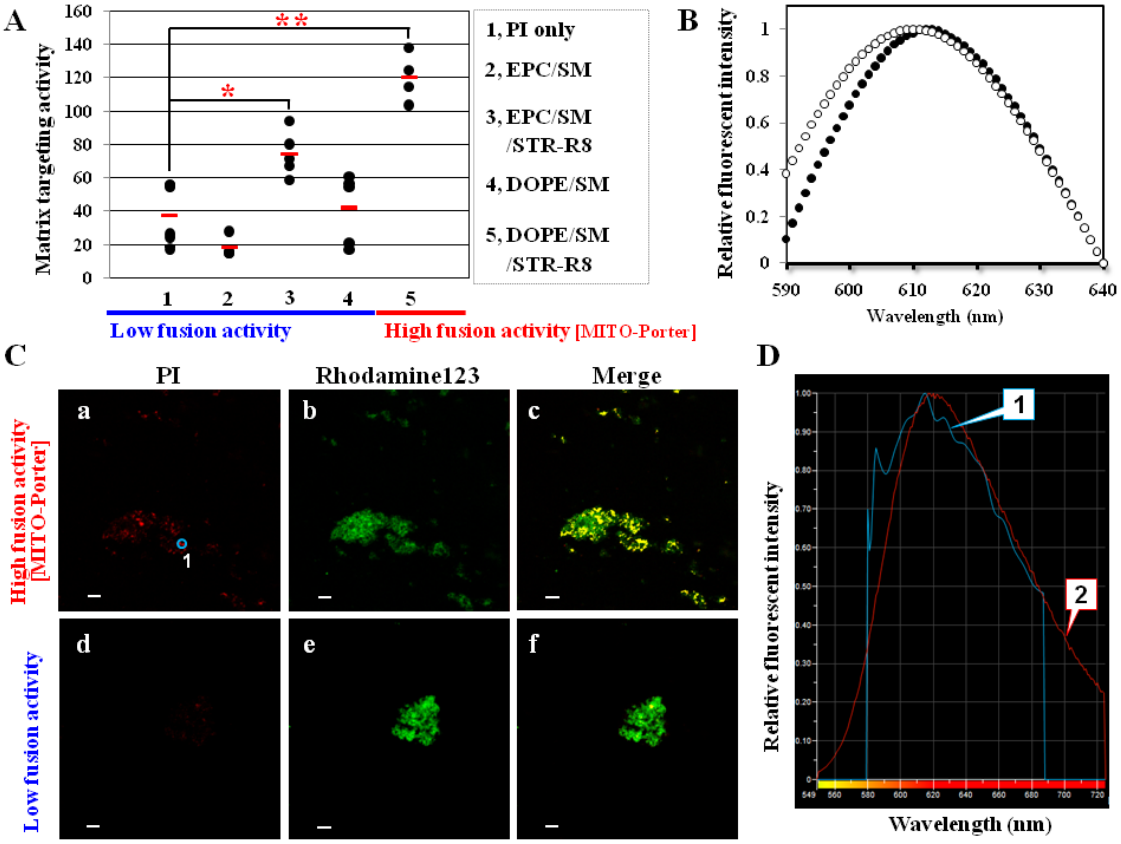
A
Matrix targeting activity
160
140
120
100
80
60
40
20
0
1
2
3
4
5
**
*
1, PI only
2, EPC/SM
3, EPC/SM /STR-R8
4, DOPE/SM
5, DOPE/SM /STR-R8
Low fusion activity
High fusion activity [MITO-Porter]
B
Relative fluorescent intensity
1
0.8
0.6
0.4
0.2
0
590
600
610
620
630
640
Wavelength (nm)
C
PI
Rhodamine123
Merge
High fusion activity [MITO-Porter]
Low fusion activity
a
b
c
d
e
f
1
D
Relative fluorescent intensity
1
2
Wavelength (nm)

Figure 3

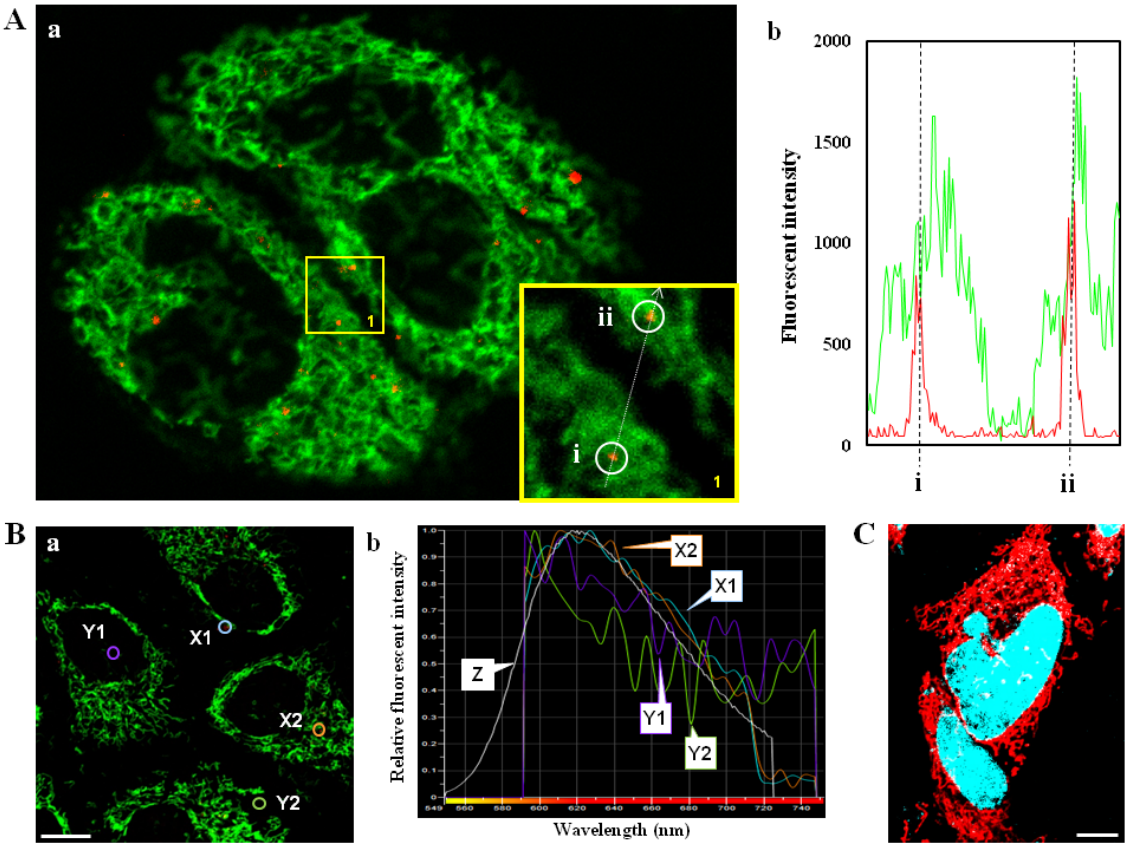
A
a
1
ii
i
1
b
2000
1500
1000
500
0
Fluorescent intensity
i
ii
B
a
Y1
X1
X2
Y2
b
Relative fluorescent intensity
X2
X1
Z
Y1
Y2
Wavelength (nm)
C

Figure 4

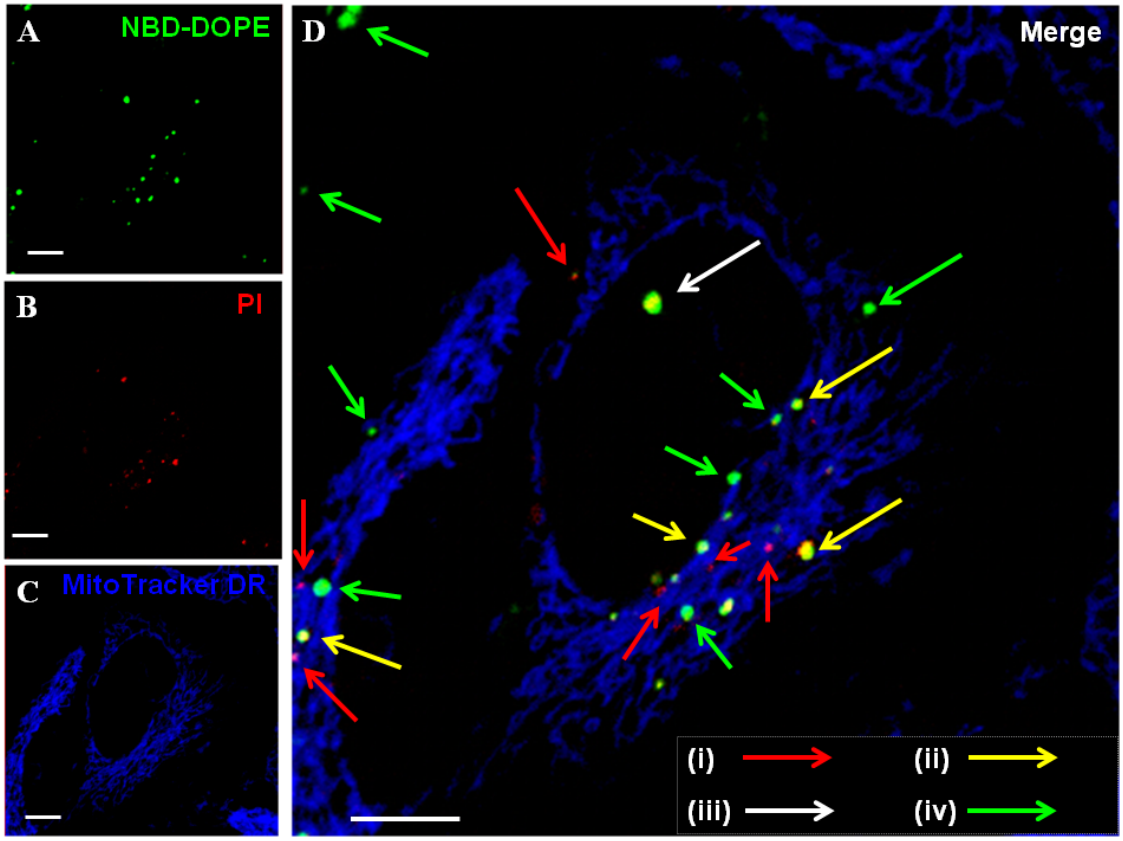

Supplemental Material

1. Materials and Methods

1.1. Isolation of mitochondria from rat liver

Mitochondria were isolated from livers obtained from adult male Wistar rats (6-8 weeks of age) essentially as described previously [1;2]. Rats were sacrificed and the livers removed after bleeding had largely subsided, and then placed in approximately 20 mL of ice-cold mitochondrial isolation buffer containing EDTA [MIB (+): 250mM sucrose, 2 mMTris–HCl, 1 mM EDTA, pH 7.4] per 10 g of liver. All subsequent steps were carried out on ice. The livers were chopped into small pieces and the suspension homogenized in a glass homogenizer (50 mL capacity) with a pestle. Three complete up and down cycles with the pestle were made. The pestle was motor-driven and operated at approximately 550 rpm. The homogenate was diluted approximately 1:3 with MIB (+) and centrifuged at 800g for 5 min. The supernatant was transferred into ice-cold tubes and centrifuged at 7,500g for 10 min. The pellets were washed twice with MIB (+), and then once with EDTA-free MIB. Concentrations of mitochondrial proteins were determined using a BCA protein assay kit. All animal

protocols were approved by the institutional animal care and research advisory committee at the Faculty of Pharmaceutical Sciences, Hokkaido University, Sapporo, Japan.

1.2. Evaluation of recovery ratio of PI

To estimate the recovery ratio, PI encapsulated in liposomes was separated from free PI by centrifugation at 30,000g for 2 hr at 25ºC. The liposome-encapsulated PI was determined by measuring the absorbance at 530 nm. The recovery ratio was calculated as follows:

Recovery ratio (%) = recovered PI / applied PI x 100 (1).

1.3. Validation for linear relationship between the amount and the fluorescent intensity of PI in the presence of mtDNA

An 80-μL aliquot of mtDNA solution (amounts of mtDNA, 0, 20, 40, 60, 80 μg) was individually mixed with PI in 20 μL of EDTA-free MIB (final PI concentration, 0.08 mg/mL). After mixing the solution, their fluorescent intensities (excitation at 535 nm and emission at 617 nm) were measured within 10 min using an FP750 instrument (JASCO, Tokyo, Japan). We also measured fluorescent intensities in the absence of PI.

1.4. Staining of nucleic acids in nuclei and mitochondria by DAPI and living cells imaging using

confocal laser scanning microscopy

Nucleic acids in nuclei and mitochondria were stained with DAPI (Fig. 3C), as previously reported [3]. HeLa cells (4 x 10^4 cells) were cultured in 35 mm glass base dishes with DMEM, which contained 10% FBS, under 5% CO_2/air at 37ºC for 24 ± 4 hr. The medium was replaced by fresh medium containing DAPI (final concentration, 15 μg/mL), and the cells were then incubated for 30 min to permit staining of the nucleic acids in the nuclei and mitochondria. After the incubation, the medium was replaced by fresh medium containing Rhodamine123 (final concentration, 100 ng/mL) and the cells were incubated for 30 min to permit staining of the mitochondria. After the incubation, the cells were washed with phenol red-free medium containing serum for observation, and then observed by CLSM (Nikon A1; Nikon Co. Ltd., Tokyo, Japan). The cells were excited with a 405 nm wavelength light from a Diode laser and a 488 nm wavelength light from an Ar laser. A series of images were obtained using a Nikon A1 microscope equipped with a water immersion objective lens (Plan Apo 60x1.20 PFS WI) and a 1st dichroic mirror (405/488/561/640). The two fluorescence detection channels were set to the following filters: 450/50 (cyan pseudo color) for nucleic acids and 525/50 (red pseudo color) for mitochondria.

2. Supplemental data

2. 1 Linear relationship between the fluorescent intensity of PI mixed with mtDNA and the amount of mtDNA (Fig. S1)

To check the linear relationship between the fluorescent intensity of PI mixed with mtDNA and the amount of mtDNA, their fluorescent intensities were measured after mixing PI with various concentrations of mtDNA (see Materials and Methods in Supplementary material).

Figure S1. Linear relationship between the fluorescent intensity of PI mixed with mtDNA and the amount of mtDNA

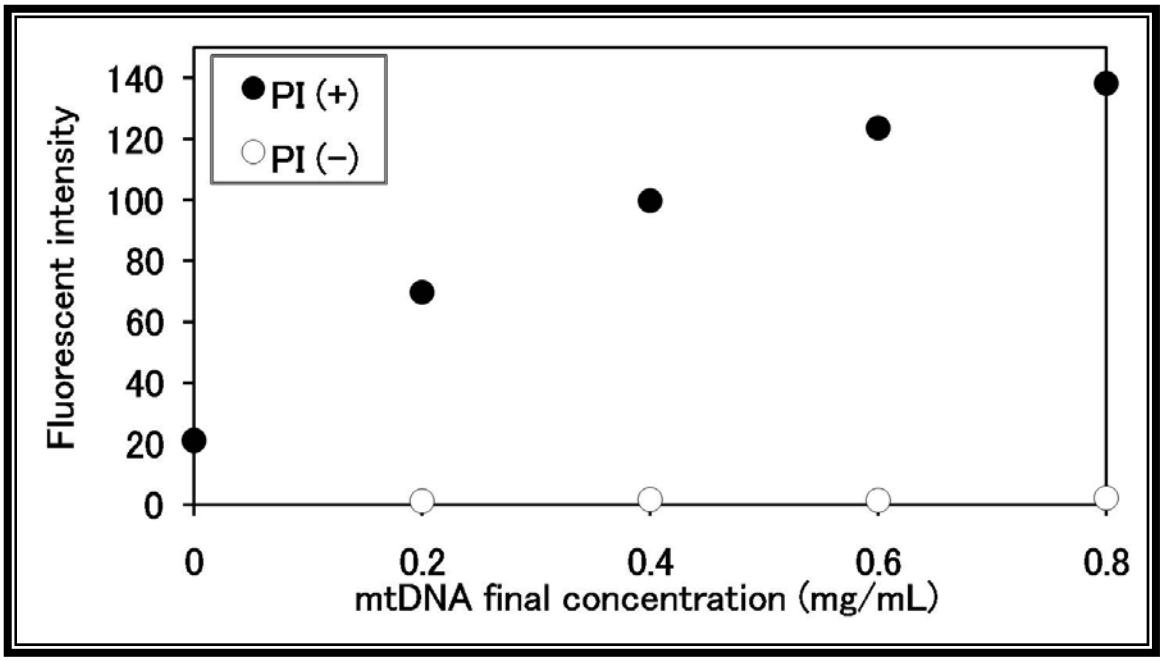

This graph shows the applied concentration of mtDNA (x-axis) against the fluorescent intensities of PI mixed with the mtDNA (y-axis). The closed and open circles represent fluorescent intensities in the presence and absence of PI, respectively. Data are represented by the mean.

2. 2 Characteristics of MITO-Porter encapsulating PI (Table S1)

We prepared liposomes encapsulating propidium iodide (PI) (see Materials and Methods for the detail in the main text). For the MITO-Porter, the lipid envelope was mitochondria-fusogenic in composition [DOPE/SM/STR-R8 (9:2:1, molar ratio)], while a non-mitochondrial fusogenic composition [EPC/SM/STR-R8 (9:2:1, molar ratio)] was used in the control lipid envelope. Their sizes, ζ potentials and mitochondrial membrane fusion activities are summarized in Table. S1. Here, we used previously reported data on mitochondrial membrane fusion activities and mitochondrial binding activities[2;4]. The recovery ratios of carries were approximately 10 %.

Table S1. Characteristics of liposomes encapsulating PI

Lipid compositions	DOPE/SM	DOPE/SM/STR-R8	EPC/SM	EPC/SM/STR-R8
Diameter (nm)	363	418	237	269
Zeta potential (mV)	-13	58	1.0	58
Mitochondrial membrane fusion activity	5	48	3	5

Data are represented by the mean (n = 1-4). EPC, egg yolk phosphatidyl choline; DOPE, 1,2-dioleoyl-sn-glycero-3-phosphatidyl ethanolamine; SM, sphingomyelin; STR-R8; stearyl octaarginine.

2. 3 Observation of isolated mitochondria using confocal laser scanning microscopy (Fig. S2)

To confirm that the red-fluorescent color observed in Fig. 2C (main text) was the result of the reaction of PI and mtDNA and not a fluorescent artifact, we observed isolated rat liver mitochondria by confocal laser scanning microscopy under various conditions, as shown in Fig. S2.

Figure S2. Observation of isolated mitochondria by confocal laser scanning microscopy

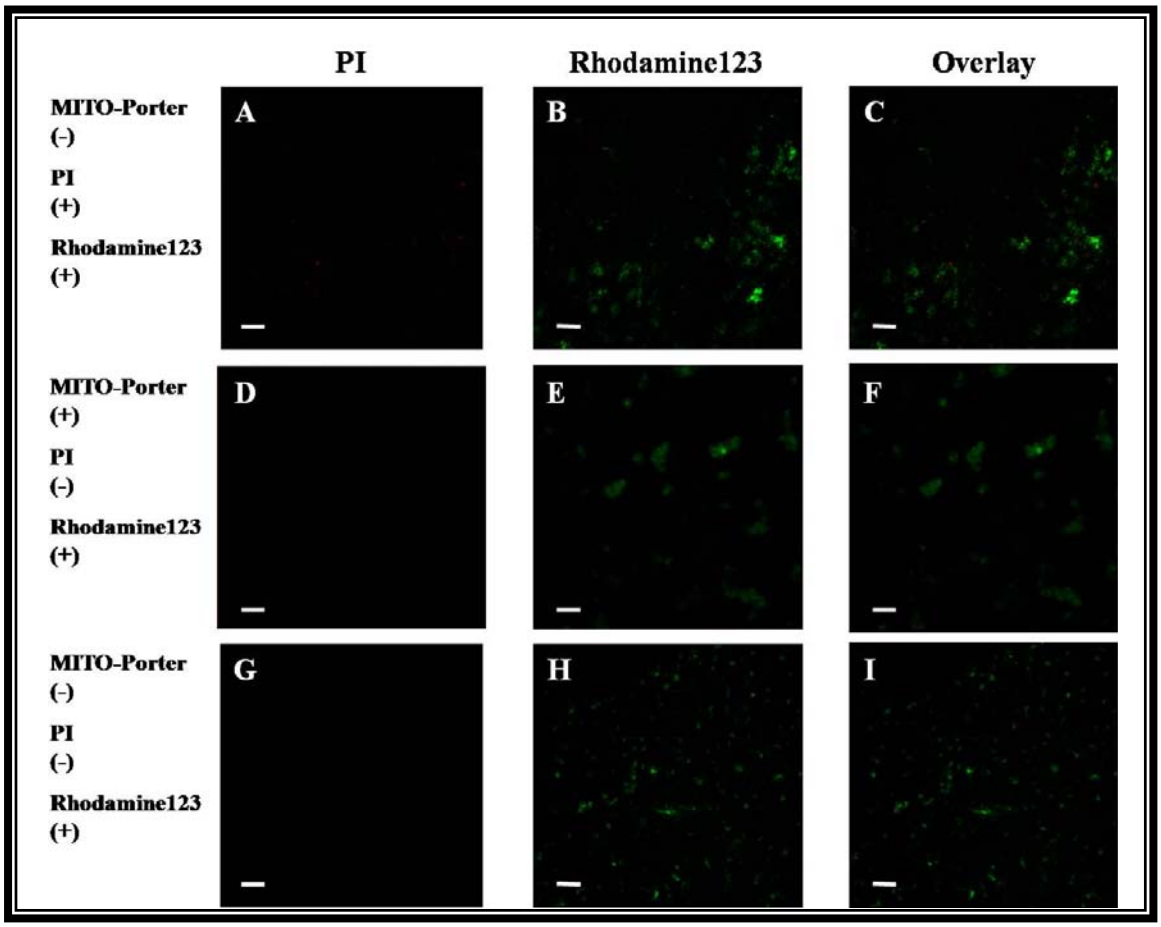

The mitochondria were observed by confocal laser scanning microscopy: (A, D, G) fluorescent images of PI, (B, E, H) fluorescent images of Rhodamine123 and (C, F, I) overlay images. Scale bars, 10 μm.

A-C, PI solution without carriers was added to isolated mitochondria. After incubation, the mitochondria were observed after staining with Rhodamine123.

D-F, MITO-Porter (DOPE/SM/STR-R8) not encapsulating PI was added to isolated mitochondria. After incubation, the mitochondria were observed after staining with Rhodamine123.

G-I, Isolated mitochondria were observed after staining with Rhodamine123 in the absence of PI and MITO-Porter.

2. 4 Observation of living cells using confocal laser scanning microscopy (Fig. S3)

To confirm that the red fluorescent color observed in Fig. 3A (main text) was the result of a reaction between PI and mtDNA and was not a fluorescent artifact, we observed living cells under various conditions by confocal laser scanning microscopy as shown in Fig. S3.

Figure S3. Observation of living cells using confocal laser scanning microscopy

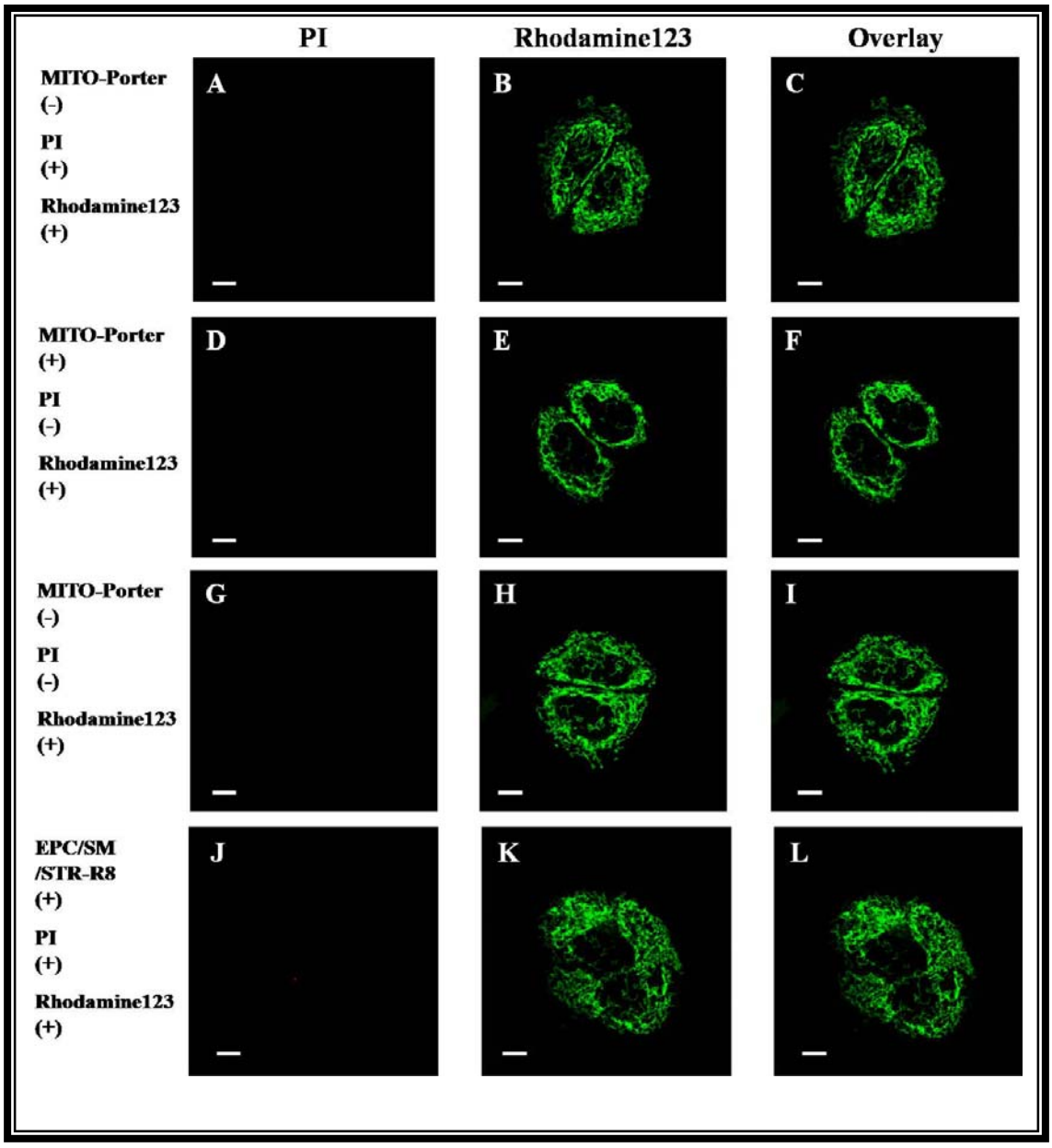

The cells were observed by confocal laser scanning microscopy: (A, D, G, J) fluorescent images of

PI, (B, E, H, K) fluorescent images of Rhodamine123 and (C, F, I, L) overlay images. Scale bars, 10 μm.

A-C, PI solution without carriers was added to HeLa cells. After incubation, the mitochondria were observed after staining with Rhodamine123.

D-F, MITO-Porter (DOPE/SM/STR-R8) not encapsulating PI was added to HeLa cells. After incubation, the mitochondria were observed after staining with Rhodamine123.

G-I, Living cells were observed after staining with Rhodamine123 in the absence of PI and MITO-Porter.

J-L, Carriers with a low mitochondrial fusion activity (EPC/SM/STR-R8) encapsulating PI were added to HeLa cells. After incubation, mitochondria were observed after staining with Rhodamine123.

References

[1] Y. Shinohara, M.R. Almofti, T. Yamamoto, T. Ishida, F. Kita, H. Kanzaki, M. Ohnishi, K. Yamashita, S. Shimizu, and H. Terada, Permeability transition-independent release of mitochondrial cytochrome c induced by valinomycin. Eur J Biochem 269 (2002) 5224-30.

[2] Y. Yamada, H. Akita, H. Kamiya, K. Kogure, T. Yamamoto, Y. Shinohara, K. Yamashita, H. Kobayashi, H. Kikuchi, and H. Harashima, MITO-Porter: A liposome-based carrier system for delivery of macromolecules into mitochondria via membrane fusion. Biochim Biophys Acta 1778 (2008) 423-32.

[3] T. Ozawa, Y. Natori, M. Sato, and Y. Umezawa, Imaging dynamics of endogenous mitochondrial RNA in single living cells. Nat Methods 4 (2007) 413-9.

[4] Y. Yamada, and H. Harashima, Mitochondrial drug delivery systems for macromolecule and their therapeutic application to mitochondrial diseases. Adv Drug Deliv Rev 60 (2008) 1439-62.